Alkaline Phosphatase-Responsive Anodic Electrochemiluminescence of CdSe Nanoparticles

ARTICLE *in* ANALYTICAL CHEMISTRY · JULY 2012

Impact Factor: 5.64 · DOI: 10.1021/ac300983t · Source: PubMed

2 AUTHORS, INCLUDING:

Hui Jiang
Southeast University (China)
120 PUBLICATIONS **1,914** CITATIONS

analytical chemistry

Article

pubs.acs.org/ac

Alkaline Phosphatase-Responsive Anodic Electrochemiluminescence of CdSe Nanoparticles

Hui Jiang and Xuemei Wang*

State Key Laboratory of Bioelectronics (Chien-Shiung Wu Laboratory), Southeast University, No. 2 Sipailou, Nanjing, 210096, People's Republic of China

ABSTRACT: Alkaline phosphatase (ALP) catalyzes the hydrolysis and transphosphorylation of a wide variety of phosphoric acid monoesters and plays an important role in clinical diagnosis. In this work, an ALP-responsive anodic electrochemiluminescence (ECL) system based on coreaction of CdSe nanoparticles (NPs) and triethylamine has been designed for facile detection of ALP. The substrate of ALP, i.e., phenyl phosphate salt, shows no effect on the ECL emission whereas its catalytic product of phenol may induce ECL inhibition. For the buffer containing phenyl phosphate, the ECL emission is found to decline in the presence of ALP with different incubation time. The mechanism investigations indicate that the deposition of the electropolymerized phenol products may compete with the electrophoretic-driven adsorption of CdSe NPs on glassy carbon electrode and induce the ECL inhibition, which can be demonstrated by scanning electron microscopy, energy dispersive spectrometry, and anodic stripping voltammetry. Therefore, an inhibition type strategy has been developed to sensitively detect ALP ranging from 0.5 to 6.4 nM (activity ca. 2−25 U/L), with a detection limit of 0.5 nM. The potential interference from the common proteins is negligible. The recovery of ALP in diluted serum samples ranges from 91 to 114%, implicating its potential applications in the complex biological matrixes.

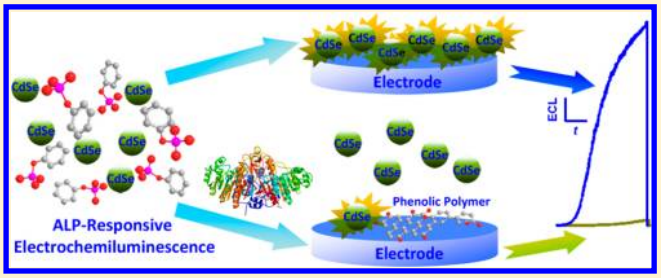

Phosphorylation-related biochemical behaviors play pivotal roles in cellular regulation and signaling processes.[1] A sensitive assay to report a switch of the phosphorylation/dephosphorylation state is crucially valuable for biomedical applications, especially for pursuing targets in novel drug design.[2] Alkaline phosphatase (ALP), which consists of a group of isoenzymes that are widespread in mammalian organisms,[3] catalyzes the hydrolysis and transphosphorylation of a wide variety of phosphoryl esters and shows great significance in clinical diagnosis. As a biomarker, abnormal levels of ALP are correlated to bone diseases, liver dysfunction, and even certain cancers.[4] Furthermore, ALP is used as an antibody binding label in immunoassays, especially enzyme-linked immunosorbent assays. Therefore, the simple and accurate detection of ALP is of high demand in the clinical field. Among the great many techniques developed to quantify ALP, fluorometry, using direct fluorescence,[5] fluorescence resonance energy transfer (FRET),[6] or time-resolved fluorescence,[7] is one of the most traditional techniques. The noble metal nanoparticle-mediated colorimetric[8,9] or surface enhanced resonance Raman scattering[10] methods have also attracted considerable concerns. In addition, electrochemical means[11−13] may be applied for ALP assays. However, current methods face some issues. For example, the synthetic fluorogenic substrates are rather expensive in despite of their high sensitivity, and the simple colorimetry usually may bring insufficient sensitivity. Therefore, diagnostic assays of ALP with high sensitivity, selectivity, speed, and cost effectiveness are still highly desirable.

This work used an alternative charming method, i.e., electrochemiluminescence (ECL) by nanoparticles (NPs), to realize ALP assays with low cost and high sensitivity. ECL is a powerful detecting tool with excellent controllability inherited from electrochemical modes and low background similar to other luminescent signals, which allows the versatile sensing applications.[14,15] Recently, the biosensors and bioassays by virtue of intrinsic ECL of a variety of nanostructures are extensively developed for diagnostic purposes, due to the efficient ECL emission and facile bioconjugation, as well as nanoenhanced signal amplification.[16,17] Generally speaking, a mass of methods involving immunoassays,[18,19] aptamer[20] or DNA[21] binding, and cytosensing[22] have been developed for sensitive detection of biological targets using cathodic ECL of nanostructures. The assays based on anodic ECL are limited, only in simple ions,[23,24] thiols,[25] and neurotransmitters.[26,27] As far as we know, no attention has been paid to detection of enzymatic catalysis relied on the direct anodic ECL of nanostructures.

The current design of the ALP-responsive system is based on two prerequisites. One is that the optimal pH of ALP activity is around 9.5, which is located in the pH range for ECL emission allowing facile detection of the ECL emission signal. The other is the selective ECL inhibition effect by the phenolic groups in ALP catalytic products but not by phenyl phosphate, an ALP

Received: April 12, 2012
Accepted: July 22, 2012
Published: July 22, 2012

dx.doi.org/10.1021/ac300983t | *Anal. Chem.* 2012, 84, 6986−6993

Scheme 1. Illustration of Principles of ALP-Responsive ECL System[a]

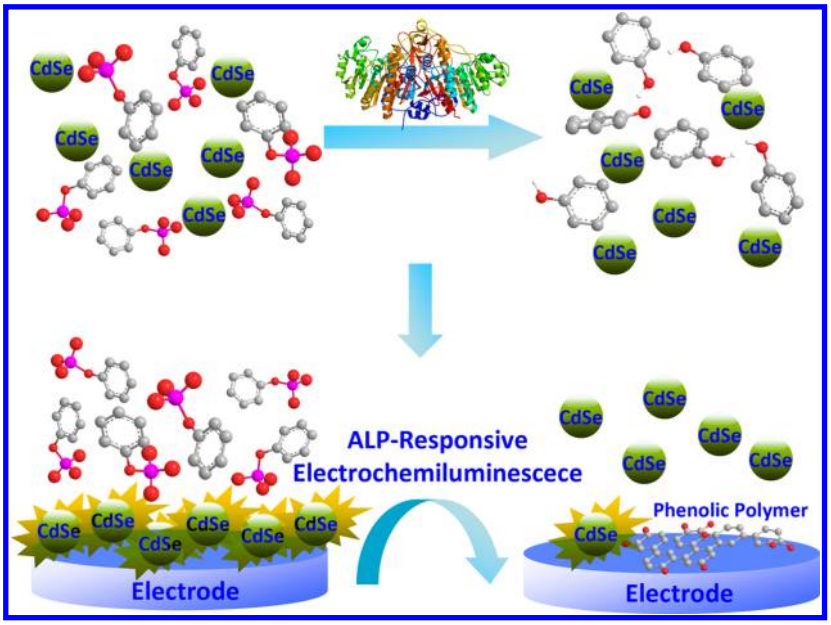

[a]The ALP-triggered hydrolyzation of PPNa to phenol will induce the formation of phenolic polymer and the subsequent ECL inhibition.

substrate. The rationale behind the ECL inhibition is demonstrated to be the competitive deposition of electropolymerized phenol (i.e., enzyme catalyzed product) with the electrophoretic-driven adsorption of CdSe NPs on glassy carbon electrode (GCE) (Scheme 1). On the basis of such inhibition, we may develop an ALP-responsive ECL system to detect the enzymatic processes sensitively and selectively. The successful assays in serum samples suggest the potential clinical prospects of the proposed system.

EXPERIMENTAL SECTION

Reagents and Apparatus. ALP (EC 3.1.3.1), bovine serum albumin (BSA), catalase (E.C. 1.11.1.6), hemoglobin (Hb), α-amylase (E.C. 3.2.1.1), and urease (E.C. 3.5.1.5) are purchased from Sigma Co. Ltd. (St. Louis, MO, USA). Se powder (99.999%), KBH_4, $CdCl_2{\cdot}2.5H_2O$, $MgCl_2{\cdot}6H_2O$, phenyl phosphate disodium (PPNa), triethylamine (TEA), thioglycerol (TG), and glycine (Gly) are of analytical grade from Sinopharm Chemical Reagent Co. Ltd. (China). The serum samples are kindly provided by the second affiliated hospital of Southeast University and stored at 4 °C with a shelf life of a week. The alkaline Gly buffer of 50 mM containing 0.5 mM Mg^{2+} was used as the ECL solution. The buffer pH can be adjusted from 8.6 to 10.6 using 1 mol L^{-1} NaOH. The Milli-Q water (a resistivity of 18.2 MΩ cm) was used throughout.

In the ECL experiments, the electrochemical signals are produced by a CHI660C electrochemical workstation (CH Instruments, USA) and the electrogenerated photons are synchronously collected with an IFFM-E analyzer (Xi'an Remax Co. Ltd., China), which combine the photomultiplier tube (PMT) with a data acquisition module. A transparent electrochemical cell, including a bare GCE (4 mm in diameter of electrode, i.e., with an apparent area of 12.56 mm^2) as the working electrode, a Pt wire as the counter electrode, a Ag/AgCl electrode as the reference electrode, and detection solution with a total volume of 2.0 mL, is placed upon the PMT (biased potential at −800 V) of the IFFM-E analyzer. The cell is equipped with a gas tube circuit and a flow rate control valve to make the gas bubbling stable (flow rate at ∼20 mL/min). The temperature is kept at 37.0 ± 1.0 °C using a recycled water bath and a temperature-controller (Lankai Co. Ltd., Shanghai, China). The amperometric *i-t* curve mode is utilized in the time course experiments, and the CV technique is applied for the potential scanning. The electrochemical impedance spectrum (EIS) measurements are carried out on an Autolab PGSTAT302N system (Eco Chemie, Netherlands), with frequency ranging from 0.01 to 10^5 Hz and amplitude of 10 mV. The scanning electron microscopy (SEM) images are obtained on an ultra plus field emission scanning electron microscopy (Zeiss, Germany) equipped with an INCA energy-dispersive X-ray spectroscopy (Oxford, England). The acceleration potential is set at 15 KV. The UV−vis spectra are scanned on a U-4100 spectrometer (Hitachi, Japan).

Preparation of TG Stabilized CdSe (CdSe/TG) NPs. The CdSe/TG NP solutions are synthesized as previously reported,[28] using Se precursors and KBH_4 as reducing agent, with a molar ratio of Cd/Se/TG = 1:0.5:2.4. The obtained clear colloidal solution is dialyzed against water three times and centrifuged to remove a morsel of precipitate. The final NP solution is stored in a refrigerator at 4 °C after it is enriched using a Nanosep ultracentrifuge device (Molecular Weight Cutoff 10K, Pall, USA). The sizes of NPs are 3.3 ± 0.5 nm, as confirmed by transmission electron microscopy (JEM-2100, JEOL, Japan). We calculate the concentration of enriched CdSe NPs (146.0 μM) by UV−vis spectra, according to the method of Peng et al.[29]

Construction of ALP-Responsive ECL System. The used buffer, namely, "standard mixture solution", represents 50 mM Gly buffer (pH 9.5) containing 14.6 μM CdSe/TG, 10 mM TEA, and 0.5 mM Mg^{2+} (ALP activator). The concept of ECL inhibition ratio ($\Delta I/I$) is used to evaluate the inhibition efficiency in ECL signals and calculated as the following equation:

$$(\Delta I/I)\% = (I - I_t)/I \times 100\%$$

dx.doi.org/10.1021/ac300983t | Anal. Chem. 2012, 84, 6986−6993

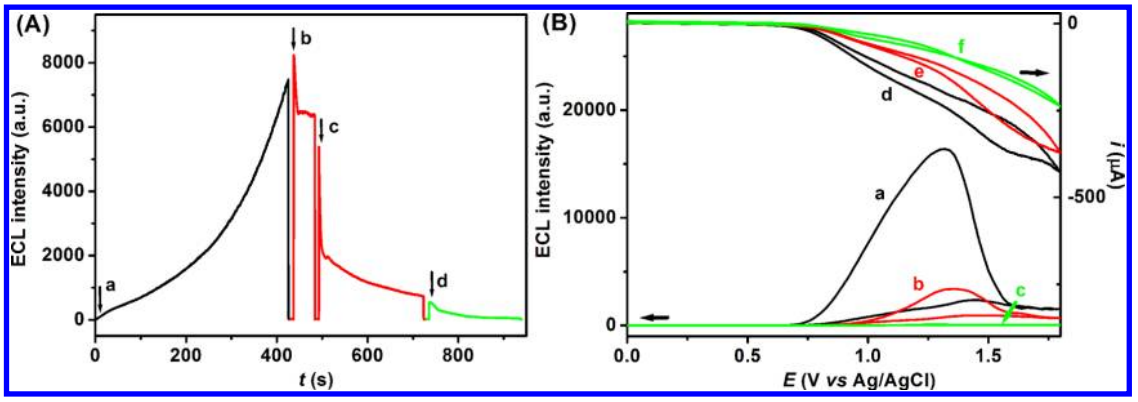

Figure 1. (A) ECL profiles recorded in standard mixture solution in the absence (a) and presence of phenol with a final concentration of 10.0 (b), 20.0 (c), and 50.0 (d) μM. The applied potential is +1.0 V. The arrows indicate successive titrations of phenol stock solution; (B) CV curves (d–f) and the corresponding ECL curves (a–c) recorded in the absence (a, d) or presence of phenol of 20.0 μM (b, e) and 50.0 μM (c, f).

where I and I_t denote the ECL intensity recorded for the control and treated samples, respectively. Before the real sample detection, the serum sample spiked with different amounts of ALP is diluted by 1000-fold in the buffer, i.e., with a final concentration of 0.1% serum. The percent recovery is calculated according to the equation: recovery % = $(A_s - A_n)/A \times 100\%$, where A_s and A_n denote amount of ALP found in spiked sample and in nonspiked sample, respectively, and A denotes the amount of ALP added. Notably, in the current case, the amount of ALP in nonspiked sample can be ignored in comparison with the spiking amount. Hence, the percent recovery is simplified as the ratio of A_s and A.

Anodic Stripping Voltammetric (ASV) Analysis. The ASV experiments are performed on the same CHI660C electrochemical workstation. In the analysis, the electrodes after each electrodeposition are fully rinsed with water and then immersed in 600 μL of 1.0 mol L^{-1} HNO_3 solution to dissolve the deposited CdSe NPs. After the release of Cd^{2+} by the intermittent ultrasonication for 1 min, 100 μL of the solution is transferred into 1.9 mL of 0.2 mol L^{-1} acetate (Ac) buffer (pH 5.3) containing 15 mg L^{-1} $Hg(Ac)_2$. The electrochemical stripping detection involves a 1 min pretreatment at +0.6 V, following a 5 min electrodeposition at −1.1 V and then stripping from −1.1 to −0.2 V using a square wave voltammetric waveform (potential step: 4 mV; frequency: 25 Hz; amplitude: 25 mV). The anodic stripping peak of Cd (II) species is located at about −0.7 V.

RESULTS AND DISCUSSION

Phenol Induced Inhibition on ECL. Recently, we have observed the dynamically enhanced ECL by the coreaction between CdSe/TG NPs and triethylamine in alkaline Gly buffer and proposed a mechanism called "potential-triggered adsorption of NPs".[28,30] As verified in these works, the CdSe NPs act as the ECL emitters and the electrophoretic movement of the negative-charged NPs toward GCE under a positive potential (for example, ~+1.0 V vs Ag/AgCl) has been demonstrated to be essential for the dynamically enhanced ECL, as indicated by eqs 1–5.[30]

$$[\mathrm{CdSe/TG}] \rightarrow [\mathrm{CdSe/TG}]\ (\mathrm{adsorbed}) \quad (1)$$

$$[\mathrm{CdSe/TG}]\ (\mathrm{adsorbed}) - e^- \rightarrow [\mathrm{CdSe/TG}]\ (h^+) \quad (2)$$

$$\mathrm{TEA} - e \rightarrow [\mathrm{TEA}^{\bullet}]^+ \rightarrow \mathrm{TEA}^{\bullet} + H^+ \quad (3)$$

$$[\mathrm{CdSe/TG}]\ (h^+) + \mathrm{TEA}^{\bullet} \rightarrow [\mathrm{CdSe/TG}]^* + \mathrm{TEA\ fragments} \quad (4)$$

$$[\mathrm{CdSe/TG}]^* \rightarrow \mathrm{CdSe/TG} + h\nu \quad (5)$$

The concentration of NPs will affect the ECL, and we have used an optimized final concentration of 14.6 μM.[28] On the basis of this principle, we have developed a novel method for the sensitive assay of serotonin, an important neurotransmitter.[31] The blockage of the "potential-triggered adsorption of NPs" by the oxidative products of serotonin results in a significant ECL inhibition effect. Actually, further research has revealed that many phenolic analogues may induce such an effect, with different responding sensitivity.

This work will first verify that the simplest one among these compounds, phenol, can also induce the ECL inhibition at a relatively high concentration.As shown in Figure 1A, with N_2 bubbling, the ECL profile recorded in "standard mixture solution" shows the ascending tendency in a few minutes (part a). Upon addition of phenol with a final concentration of 10.0 μM after 7 min (part b), the ECL intensity may decrease by ca. 20%. This concentration is 25-fold higher than that of serotonin (~0.4 μM) with the same inhibition efficiency,[31] demonstrating that the inhibition is relatively inefficient for phenol. The inhibition enhances sharply after injection of the second 10.0 μM of phenol (part c), and the ECL emission may almost be completely quenched in the presence of phenol of 50.0 μM (part d). The ECL emission has also been recorded using cyclic voltammetric (CV) scanning mode (0–+1.8 V vs Ag/AgCl). A similar decrease in ECL peak intensity appears, with a constant peak potential around +1.3 V (a–c, Figure 1B). In the corresponding CV curves (d–f, Figure 1B), the augmented currents above +0.8 V reflect ECL coreactions between NPs on the GCE surface and TEA radicals, as indicated in eqs 2–4. Compared with the case without addition of phenol (curve d), the currents sharply decrease with the increasing phenol concentrations (curves e and f), implicating the attenuation in electronic exchange during the ECL coreactions. From these results, it can be concluded that the ECL signals can be inhibited and even completely quenched by phenol of concentrations at the level of 10^{-5} M. Chen et al. have investigated the "electrochemical oxidation inhibiting" mechanism for phenol-induced inhibition of the $[Ru(bpy)_3]^{2+}$-TEA system.[32] The inhibition is considered to be attributed to the significant change of IR drop in the thin-layer flow cell by the

dx.doi.org/10.1021/ac300983t | Anal. Chem. 2012, 84, 6986–6993

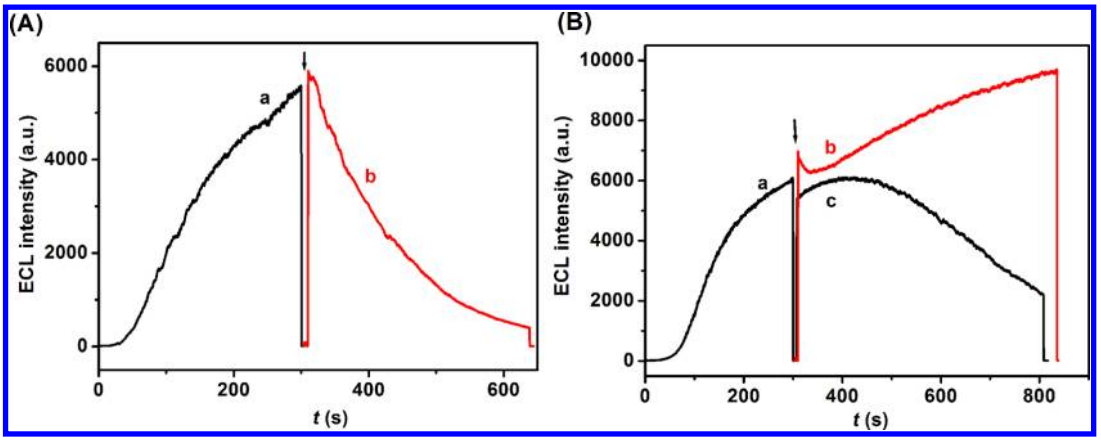

Figure 2. (A) ECL profile recorded in standard mixture solution containing PPNa of 1.0 mM (curve a) and after fast injection of ALP of 6.4 nM (curve b). (B) ECL profile recorded in standard mixture solution containing ALP of 6.4 nM (curve a) and after fast injection of 2.0 mM HPO_4^{2-} (curve b) or PPNa of 1.0 mM (curve c). Both arrows indicate the injection of the corresponding substances.

electroactive inhibitor. In our case, however, the inhibition processes may be quite different from this mechanism, as demonstrated in the following research.

Investigation of ALP-Responsive ECL Inhibition. The inhibition effect by phenol offers an opportunity to design an ALP-responsive ECL system, since phenol is a product of ALP catalyzed hydrolysis when PPNa as substrate is used. However, to fabricate such a specific system, the possible influence from the biochemical matrixes should be evaluated in detail. The first potential interfering agent is PPNa, the substrate. For standard mixture solution containing PPNa, the ECL time course (curve a, Figure 2A) shows a similar profile compared to the solution without PPNa (Figure 1A). It is notable that in this case the concentration of PPNa may reach up to 1.0 mM and is much higher than the quenching concentration of phenol (50 μM). Therefore, the inhibition effect by the substrate can be fully excluded. Subsequently, the introduction of 6.4 nM ALP results in a rapid decrease in ECL signal (curve b, Figure 2A). Such a decrease may originate from either ALP catalytic products (including phenol and HPO_4^{2-} ion) or ALP itself. However, compared with the ECL profile obtained in standard mixture solution (curve a, Figure 1A), no significant difference has been observed for that in the same solution containing 6.4 nM ALP (curve a, Figure 2B), suggesting the absence of interference from ALP itself. At the same time, the ECL track in ALP-containing standard mixture solution keeps ascending upon addition of HPO_4^{2-} at 300 s (curve b, Figure 2B), demonstrating the negligible inhibition by phosphate. In contrast, further addition of PPNa to ALP-contained standard mixture solution at 300 s leads to the declining ECL emission (curve c, Figure 2B), implying the significant inhibition effect by generated phenol. These results demonstrate that, although a lot of species may be involved in the ECL processes, phenol is the only molecule that mediates ECL emission. Therefore, using standard mixture solution containing PPNa of a certain concentration, an ECL system with specific ALP response may be successfully constructed.

The ALP-responsive ECL system can be further investigated to provide more detailed mechanism information. The interfacial electronic transfer kinetics usually plays a decisive role in ECL processes. For example, in our previous work,[30] the adsorption behaviors on GCE surface are essential to the following ECL burst. Here, the electrochemical behaviors of GCE surfaces upon various pretreatments have been inspected by the EIS technique. From the Nyquist plots in Figure 3, the charge transfer resistance (R_{ct}) for a bare GCE is only 50 Ω

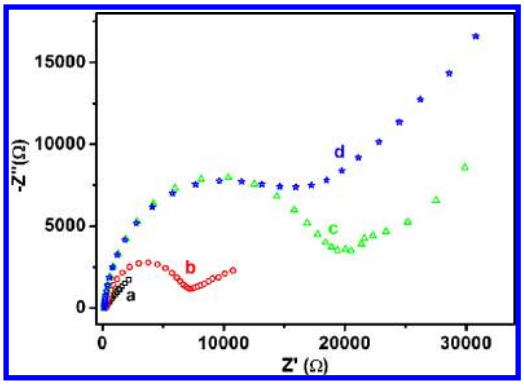

Figure 3. The Nyquist plot for bare GCE (a, hollow square), GCE after electrodeposition in standard mixture solution containing PPNa of 0.5 mM (b, hollow circle), in standard mixture solution containing 50.0 μM phenol (c, hollow triangle), and in standard mixture solution containing PPNa of 0.5 mM and ALP of 2.56 nM, with a preincubation time of 3 min at 37 °C (d, hollow star). All deposition time is 5 min. The electrolyte is 5 mM $[Fe(CN)_6]^{3-/4-}$.

(curve a). After a 5 min electrodeposition in standard mixture solution containing PPNa of 0.5 mM, the GCE shows an increasing R_{ct} of 7.1×10^3 Ω (curve b), corresponding to the electric field-driven adsorption of the semiconductor CdSe NPs. When the bare GCE is treated the same in standard mixture solution containing 50.0 μM phenol, it renders a ~3-fold higher R_{ct} of 2.0×10^4 Ω (curve c). If the bare GCE is incubated with standard mixture solution containing PPNa and ALP for 3 min and then subjected to the 5 min electrodeposition, a similar R_{ct} value of 1.9×10^4 Ω can be obtained (curve d). The ultrahigh R_{ct} should be attributed to the attached organic insulators through electropolymerization of phenol on GCE. We predict that electropolymerization of phenol will also compete with potential enhanced adsorption of CdSe NPs and block the proposed ECL emission cycle, resembling the processes verified for serotonin in our previous work.[31]

To validate the hypothesis, the GCE surfaces upon the above treatments have been further characterized by SEM. When bare GCE is immersed in standard mixture solution containing

dx.doi.org/10.1021/ac300983t | Anal. Chem. 2012, 84, 6986−6993

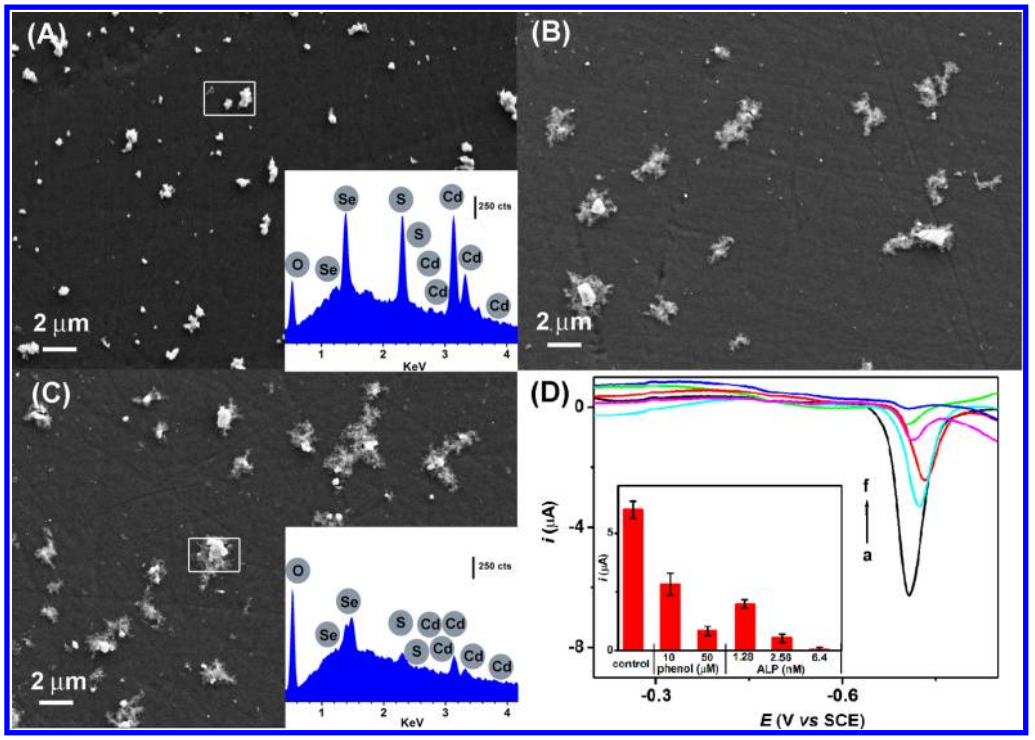

Figure 4. The SEM of GCE (magnification ×10 000) after electrodeposition in standard mixture solution containing PPNa of 0.5 mM (A), or containing 30 μM phenol (B), or containing PPNa of 0.5 mM and ALP of 2.56 nM, with a preincubation time of 3 min (C). A and C inset: EDS of a rectangle region indicated by white border; (D) ASV curves of electrodeposited GCE in standard mixture solution containing 10 (b) and 50 (d) μM phenol, or containing PPNa of 0.5 mM and 1.28 (c), 2.56 (e), or 6.4 (f) nM ALP, with a preincubation time of 3 min. The electrodeposited GCE in standard mixture solution containing PPNa of 0.5 mM is used as control (a). D inset: the comparison of the stripping currents. All deposition conditions are same as those described in Figure 3.

PPNa and incubated with a potential of +1.0 V for 5 min, submicrometer sized bright and irregular spots emerge on GCE surface (Figure 4A), indicating the adsorption of NP aggregates. After treatment in standard mixture solution containing phenol, the SEM image mainly shows flocculent aggregates (Figure 4B), besides a small quantity of bright spots like those appearing in Figure 4A. Similar surface modification can be obtained on GCE treated surfaces using standard mixture solution containing both PPNa and ALP (Figure 4C). The latter two images reflect the electropolymerization of phenol on GCE surface, which hampers the enrichment of NPs. The EDS results strongly support the above consequence. After treatment in standard mixture solution containing only PPNa, the calculated atom contents of Cd and Se reach 0.29% and 0.14%, respectively (from a random region of 3 μm × 2 μm, Figure 4A inset). The atom ratio is ~1:0.48 for Cd/Se and coincident with the ratio in CdSe NP solution (Cd/Se 1:0.5), suggesting the almost intact deposition of NPs on GCE. For the treatment in standard mixture solution containing both PPNa and ALP, the EDS pattern shows very weak Cd and Se peaks (Figure 4C inset). The estimated Cd content decreases to 0.05% and is only 17% of that containing only PPNa. Simultaneously, the oxygen content increases dramatically by 65%, which originates from the electropolymerized phenol species. These results completely demonstrate the significant competitive relationships between electropolymerization of phenol and adsorption of CdSe NPs.

Furthermore, to quantitatively discuss the surface modification of CdSe NPs upon these treatments, the Cd adsorption on GCE is analyzed using the ASV technique (Figure 4D). For treatment in standard mixture solution containing PPNa of 0.5 mM (control group), the mean stripping current for Cd (II) is 5.99 ± 0.37 μA (curve a), corresponding to the effective adsorption of CdSe NPs. As to the system containing 10 μM (curve b) and 50 μM (curve d) of phenol, the current is only 47.2% and 13.8% of that obtained for the control group, respectively, indicating the great decrease in the adsorbance of CdSe NPs. The decrease should be induced by the above-mentioned electropolymerized products of phenol, which impedes the electrochemical driven adsorption of CdSe NPs and inhibits the accompanied efficient ECL emission. For treatments in standard mixture solution containing PPNa and 1.28 nM (curve c) or 2.56 nM (curve e) or 6.4 nM ALP (curve f), the stripping currents are 33.1%, 8.8%, and 1.0% of the current for control group, respectively. The decreasing amplitude is dose-dependent, i.e., the higher ALP activity will induce the lower adsorbance of CdSe NPs, which is consistent with the phenol groups. For the case using 6.4 nM ALP, the stripping current is very weak, showing only trace Cd residues on GCE. Generally speaking, PPNa shows little influence on the adsorption of CdSe NPs on GCE even at a high concentration, while phenol largely inhibits the adsorption process, which allows the excellent performances of the ALP-responsive ECL system. The whole principle can be illustrated as Scheme 1. The ECL emission is dependent on the potential-controlled adsorption of CdSe NPs on GCE, and phenyl phosphate hardly affects the adsorption. The presence of ALP induces the production of phenol, which then electropolymerizes on GCE and competes with the NPs adsorption, thus resulting in the ECL inhibition.

Detection Optimization. We have considered the possible factors that mediate the ECL inhibition effect, including the

dx.doi.org/10.1021/ac300983t | *Anal. Chem.* 2012, 84, 6986−6993

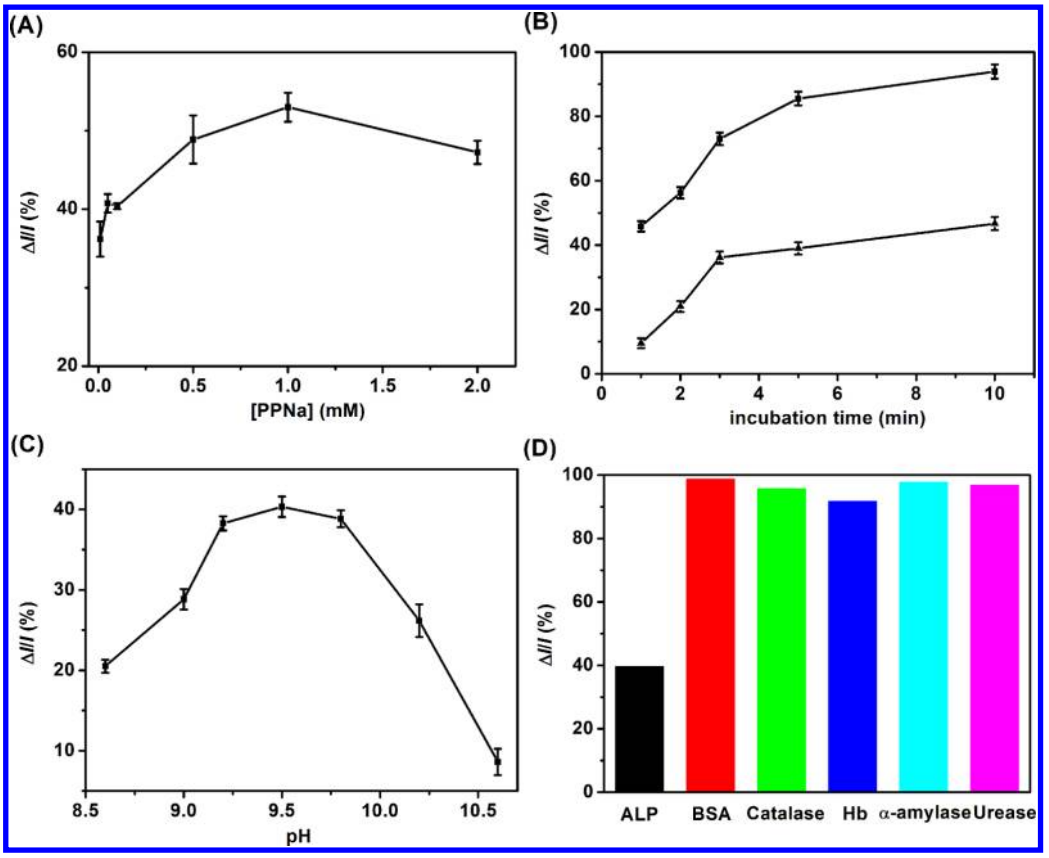

Figure 5. (A) The effect of PPNa concentration on ECL inhibition ratio ($\Delta I/I$) in standard mixture solution containing ALP of 2.56 nM, with a preincubation time of 1 min; (B) the influence of preincubation time on $\Delta I/I$ in standard mixture solution containing PPNa of 0.5 mM and ALP of 1.28 nM (triangle) or 2.56 nM (cube); (C) pH effect on $\Delta I/I$ in 50 mM Gly buffer (pH 8.6−10.6) containing CdSe/TG (14.6 μM), TEA (10 mM), PPNa (0.5 mM), and ALP (1.28 nM), with a preincubation time of 3 min; (D) influence of ECL emission by ALP (1.28 nM), BSA (300 nM), catalase (40 nM), Hb (40 nM), amylase (320 nM), and urease (40 nM), with a 3 min preincubation.

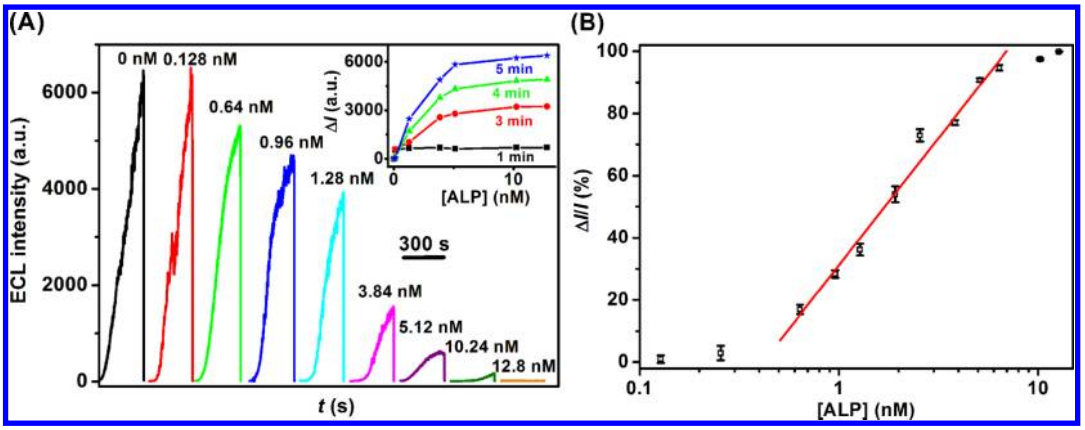

Figure 6. (A) The inhibition of ECL profiles (recorded for 5 min) induced by different concentrations of ALP ranging from 0 to 12.8 nM, inset: the plot of ECL variance (ΔI) against ALP concentration recorded at 1 (cube), 3 (dot), 4 (triangle), or 5 min (star); (B) the corresponding calibration plot of the ECL inhibition ratio against ALP concentration.

concentration of PPNa, the preincubation time, and the buffer pH. It is well-known that the amount of substrate in an enzyme catalytic reaction should be largely excessive to ensure the rapid and efficient generation of products. We have investigated the PPNa concentration ranging from 0.01 to 2.0 mM. As shown in Figure 5A, in the presence of ALP of 1.28 nM, the ECL inhibition ratio using PPNa of less than 0.1 mmol L^{-1} (~40%) is lower than those using above 0.5 mmol L^{-1} (~50%). Hence, a PPNa concentration of 0.5 mmol L^{-1} may guarantee the sufficient consumption of substrate in the current case.

The enzymatic dynamics are of great concern to meet the following detection purpose. In our strategy, all ALP samples are preincubated with standard mixture solution containing 0.5 mmol L^{-1} PPNa at 37 °C for a certain time before initiating the 5 min *i-t* scan. Obviously, the prolonged "preincubation" time means generation of more amount of phenol, which is favorable for improvement in ALP responsive sensitivity. However, the

dx.doi.org/10.1021/ac300983t | *Anal. Chem.* 2012, 84, 6986−6993

ALP catalysis will be prevented by the negative feedback from high concentration of phenol. Undoubtedly, using ALP of 1.28 or 2.56 nM, the ECL inhibition ratio initially increases with the time and then tends to be stable in 3−5 min (Figure 5B). A preincubation time of 3 min may be appropriate.

Additionally, the pH values are also important to the enzymatic processes. In this case, the ECL inhibition ratio reaches a plateau from pH 9.2 to 9.8, with a summit of ∼38% at pH 9.5 (Figure 5C) and decreases rapidly in both sides out of this pH range. As known, ALP shows a maximum activity in the range of 9.5−9.8. The consistent range suggests that the ECL inhibition ratio can be used as a potential index to illuminate ALP activity. Finally pH 9.5 is selected in the detection steps.

Sensitive Detection of ALP. On the basis of the ALP-responsive ECL inhibition system, we may develop a facile method to detect ALP sensitively. With the above optimized detection conditions, the higher ALP activity will catalyze the generation of higher concentration of phenol in definite time and thus induce the increasing ECL inhibition efficiency. Using *i-t* mode with a constant potential of +1.0 V, the ECL profiles in response to different concentrations of ALP are exhibited as Figure 6. As designed, the ECL ascending rates decreased upon the increasing amount of ALP (0−12.8 nM) in the detection solution (Figure 6A). The ECL variance (ΔI, i.e., the ECL difference between cases in the absence and presence of ALP) recorded at 1, 3, 4, and 5 min are shown in Figure 6A inset, respectively. Evidently, the prolonged scanning time will lead to the larger ΔI and favor the improved detection sensitivity. Finally, a detection time of 5 min is selected and the ECL inhibition ratios at 5 min are plotted vs ALP concentration (Figure 6B). A linear relationship (R = 0.991) can be fitted in the range of 0.5−6.4 nM (activity ca. 2−25 U/L) (1 U denotes the release of 1.0 μmol phenol per minute at 37 °C), and the detection limit is calculated to be 0.5 nM (S/N = 3). The detection limit is 1−3 order lower than those obtained using colormetric[8] (ca. 0.34 μM), FRET[6] (10 U/L), and time-resolved fluorometric[7] (4 μM) methods. Besides, the substrate of phenyl phosphate is much cheaper than *p*-nitrophenyl phosphate and other artificially designed substrates, indicating the low cost of the proposed method. This system is also simpler than the bienzyme system used for electrochemical assays of ALP.[13]

The interferences from the common proteins in the biological samples have also been examined. BSA, catalase, Hb, α-amylase, and urease do not induce significant ECL inhibition at concentrations above 40 nM (Figure 5D), which correspond to 30−250-fold ALP concentration (1.28 nM) that triggers a 40% ECL inhibition. Higher concentrations of catalase and Hb may cause ECL inhibition due to the effective energy transfer from semiconductor NPs to porphyrin antennae in their active sites.[33]

The detection of ALP spiked in the serum samples has also been investigated by the proposed strategy. Considering the abundant matrix proteins in serum, all samples are diluted in the Gly buffer by 1000-fold before detection, with a final concentration of 0.1% (v/v) serum. The percent recovery is acceptable in as-prepared detection solution, with 91% for spiking ALP of 0.64 nM [average found/added (pmol): 1.16/1.28], 114% for spiking ALP of 1.28 nM [average found/added (pmol): 2.92/2.56], and 108% for spiking ALP of 3.84 nM [average found/added (pmol): 8.30/7.68], respectively. These results indicate the promising applications in the complex biological matrixes.

CONCLUSION

In summary, we have successfully designed an ALP-responsive ECL system based on the specific inhibition on anodic ECL of CdSe NPs by phenol, the ALP catalytic product. The further investigation supports the hypothesis of competition between the electrophoretic-driven adsorption of CdSe NPs and deposition of electropolymerized phenol products on electrodes. An inhibition type strategy has been developed to sensitively detect ALP concentrations with low detection limit. The proposed method may exclude potential interference from common proteins and show acceptable coincidence in diluted serum samples, implying the detection prospects in complex biological matrixes.

AUTHOR INFORMATION

Corresponding Author

*E-mail: xuewang@seu.edu.cn. Tel/Fax: +86-25-83792177.

Notes

The authors declare no competing financial interest.

ACKNOWLEDGMENTS

This research has been supported by the Ministry of the Science and Technology of China (2010CB732404), the National Science Foundation of China (20905012, 21175020), Doctoral Fund of Ministry of Education of China (20090092110028), and the Visiting Scholar Foundation of State Key Lab of Electroanalytical Chemistry in Changchun Institute of Applied Chemistry.

REFERENCES

(1) Julien, S. G.; Dube, N.; Hardy, S.; Tremblay, M. L. *Nat. Rev. Cancer* **2011**, *11*, 35−49.
(2) Noble, M. E.; Endicott, J. A.; Johnson, L. N. *Science* **2004**, *303*, 1800−1805.
(3) Harris, H. *Clin. Chim. Acta* **1990**, *186*, 133−150.
(4) Ooi, K.; Shiraki, K.; Morishita, Y.; Nobori, T. *J. Clin. Lab. Anal.* **2007**, *21*, 133−139.
(5) Levine, M. N.; Raines, R. T. *Anal. Biochem.* **2011**, *418*, 247−252.
(6) Jia, L.; Xu, J. P.; Li, D.; Pang, S. P.; Fang, Y.; Song, Z. G.; Ji, J. *Chem. Commun.* **2010**, *46*, 7166−7168.
(7) Schrenkhammer, P.; Rosnizeck, I. C.; Duerkop, A.; Wolfbeis, O. S.; Schaferling, M. *J. Biomol. Screen.* **2008**, *13*, 9−16.
(8) Choi, Y.; Ho, N. H.; Tung, C. H. *Angew. Chem., Int. Ed.* **2007**, *46*, 707−709.
(9) Wei, H.; Chen, C.; Han, B.; Wang, E. *Anal. Chem.* **2008**, *80*, 7051−7055.
(10) Ingram, A.; Moore, B. D.; Graham, D. *Bioorg. Med. Chem. Lett.* **2009**, *19*, 1569−1571.
(11) Kazakeviciene, B.; Valincius, G.; Kazemekaite, M.; Razumas, V. *Electroanalysis* **2008**, *20*, 2235−2240.
(12) Murata, T.; Yasukawa, T.; Shiku, H.; Matsue, T. *Biosens. Bioelectron.* **2009**, *25*, 913−919.
(13) Serra, B.; Morales, M. D.; Reviejo, A. J.; Hall, E. H.; Pingarron, J. M. *Anal. Biochem.* **2005**, *336*, 289−294.
(14) Forster, R. J.; Bertoncello, P.; Keyes, T. E. *Annu. Rev. Anal. Chem.* **2009**, *2*, 359−385.
(15) Miao, W. *Chem. Rev.* **2008**, *108*, 2506−2553.
(16) Lei, J.; Ju, H. *TrAC, Trends Anal. Chem.* **2011**, *30*, 1351−1359.
(17) Huang, H.; Li, J.; Zhu, J. *Anal. Methods* **2011**, *3*, 33−42.
(18) Lin, D.; Wu, J.; Yan, F.; Deng, S.; Ju, H. *Anal. Chem.* **2011**, *83*, 5214−5221.
(19) Li, L.; Liu, K.; Yang, G.; Wang, C.; Zhang, J.; Zhu, J. *Adv. Funct. Mater.* **2011**, *21*, 869−878.
(20) Wang, J.; Shan, Y.; Zhao, W.; Xu, J.; Chen, H. *Anal. Chem.* **2011**, *83*, 4004−4011.

(21) Divsar, F.; Ju, H. *Chem. Commun.* **2011**, *47*, 9879−9881.
(22) Han, E.; Ding, L.; Jin, S.; Ju, H. *Biosen. Bioelectron.* **2011**, *26*, 2500−2505.
(23) Liu, X.; Guo, L.; Cheng, L.; Ju, H. *Talanta* **2009**, *78*, 691−694.
(24) Zhang, L.; Shang, L.; Dong, S. *Electrochem. Commun.* **2008**, *10*, 1452−1454.
(25) Wang, Y.; Lu, J.; Tang, L.; Chang, H.; Li, J. *Anal. Chem.* **2009**, *81*, 9710−9715.
(26) Liu, X.; Jiang, H.; Lei, J.; Ju, H. *Anal. Chem.* **2007**, *79*, 8055−8060.
(27) Zhao, J.; Chen, M.; Yu, C.; Tu, Y. *Analyst* **2011**, *136*, 4070−4074.
(28) Jiang, H.; Wang, X. M. *Electrochem. Commun.* **2009**, *11*, 1207−1210.
(29) Yu, W. W.; Qu, L. H.; Guo, W. Z.; Peng, X. G. *Chem. Mater.* **2003**, *15*, 2854−2860.
(30) Jiang, H.; Wang, H.; Wang, X. M. *Electrochim. Acta* **2010**, *56*, 553−558.
(31) Jiang, H.; Wang, X. M. *Chem. Asian J.* **2011**, *6*, 1533−1538.
(32) Chi, Y. W.; Dong, Y. Q.; Chen, G. N. *Anal. Chem.* **2007**, *79*, 4521−4528.
(33) Zenkevich, E. I.; Sagun, E. I.; Knyukshto, V. N.; Stasheuski, A. S.; Galievsky, V. A.; Stupak, A. P.; Blaudeck, T.; von Borczyskowski, C. *J. Phys. Chem. C* **2011**, *115*, 21535−21545.